Improved Chan Algorithm Based Optimum UWB Sensor Node Localization Using Hybrid Particle Swarm Optimization

YEDIDA VENKATA LAKSHMI[1], PARULPREET SINGH[1], MOHAMED ABOUHAWWASH[2,3], SHUBHAM MAHAJAN[4], (Member, IEEE), AMIT KANT PANDIT[4], (Senior Member, IEEE), AND ABEER B. AHMED[5,6]

[1]Department of Electrical and Electronics Engineering, Lovely Professional University, Phagwara, Punjab 144402, India
[2]Department of Mathematics, Faculty of Science, Mansoura University, Mansoura 35516, Egypt
[3]Department of Computational Mathematics, Science, and Engineering (CMSE), Michigan State University, East Lansing, MI 48824, USA
[4]Shool of Electronics and Communication, Shri Mata Vaishno Devi University, Katra 182320, India
[5]Lecturer at Department of Computers & Information Systems, Sadat Academy for Management Sciences, Cairo 12577, Egypt
[6]Software Engineering Department, College of Computing and Information Technology, Arab Academy for Science, Technology and Maritime, Cairo 12577, Egypt

Corresponding authors: Parulpreet Singh (parulpreet.23367@lpu.co.in) and Shubham Mahajan (mahajanshubham2232579@gmail.com)

ABSTRACT The localization of Wireless sensor networks (WSNs) has been recognized as one of the most challenging problems to overcome. Thus, much work has been given to solving this difficult problem. In emergency services, navigational systems, civil/military surveillance etc., locating the signal source in a WSN is essential. A novel approach for sensor node localization using range-based localization methodology has been proposed to overcome this issue. The problem is expressed in the form of a maximum probability distribution function. The use of an RSSI-based Time Difference of Arrival (TDOA) measurement model, along with the Chan algorithm, is used to find the coordinates of unknown nodes has been proposed. With the help of ultra-wideband, this research aims to develop new and precise localization algorithms for wireless sensor networks (WSNs). This work offers localization using two-hybrid localization algorithms, i.e., ELPSO (Ensemble learning particle swarm optimization) and PSO- BPNN (Back-propagation neural network optimized by particle swarm optimization). Further, the error optimization accuracy has been compared between those algorithms using simulations. The proposed techniques consistently offer a better localization accuracy than the conventional algorithms available in the literature. The new localization methods with optimal techniques reduce the error value to a minimal distance. The distance value of localization error is nearly 2.7cms compared to other designs from the literature. It is noted as significantly less.

INDEX TERMS Chan algorithm, Kalman filter, PSO, range based, 3D-node localization.

I. INTRODUCTION

The utilization of wireless sensor networks (WSNs) in a range of applications. In this paper, the use of hybrid algorithms for anchor-based node localization in UWB indoor networks is investigated. This technology has been created by several different researchers. It has become increasingly popular to use GPS and maps to locate a person in recent years. Buildings are a barrier to GPS location signals that becomes GPS unable to function indoors. [1]. A number of indoor localization methods have been created as a result of GPS location inaccu-

racies [2]–[7]. These include infrared, Wi-Fi, Bluetooth and ZigBee techniques as well as radio frequency (RFID)/ultra-wideband technology. The use of UWB technology increases the durability.

The use of UWB-enabled devices and the deployment of UWB signals are still necessary. Sensor networks are one of the most significant technological developments of modern years. When it comes to satisfying sophisticated communication and computer technology needs and specifications, WSN has shown to be a very reliable and practical technology. Sensor nodes collect data, which is then communicated to the central unit. Sensor nodes are typically created by a single move that includes a specific number of sensors. There are

The associate editor coordinating the review of this manuscript and approving it for publication was Geng-Ming Jiang.

numerous reasons why sensors fail to provide expected data in a wireless sensor network (WSN). The presence of a sensor node negatively influences the location or tracking system since it does not give the required positional data. When an absolute sensor becomes unavailable, a neural network method can temporarily replace it using time-series predictions. There's a problem with the system's fault mode operation. After learning and measuring RSSI, the neural network calculates the X and Y coordinates of the objective.

A virtual sensor and a real one is theoretically equivalent, thus this paper analysis their effects on the system when both are active and when only the virtual sensor is active.

Low-accuracy narrowband transducers influence ultrasonic indoor positioning. There is no real-time location capability with RFID [6], and the positioning precision is just about 5 meters. Unlike other wireless technologies, UWB does not rely on a carrier network [7]. Ultra-wideband signals can be transmitted using nanosecond or nanosecond signals, which allow the ultra-wideband signal to have a high resolution and higher location precision while utilizing less energy and having compact network systems. Therefore, UWB technology is particularly well-suited for indoor real-time location that is both dependable and accurate. Even though UWB is convenient, it still has certain limitations of accuracy, particularly when it comes to 3D indoor localization [8], [9]. This challenge can be solved by improving ranking algorithms or positioning algorithms in hardware. There are still a number of challenges to overcome, such as multipath fading and shadowing effects. Over time, the cost of network development and equipment installation will likewise rise substantially as a result of these changes.

PSO is a well-known optimization method that is based on conventional instinctive networks, that is why it has become so successful. An entire swarm of particles flies and searches in a limited area at a given pace, attempting to locate the ideal location in pattern [10], [11]. Simple implementation and high performance have made PSO a popular tool for solving real-time scheduling and engineering challenges. Although most UWB indoor localization systems use only one PSO algorithm, our technique attempts a better solution by integrating multiple PSO algorithms. As a result of our observations, we believe that it is difficult to attain flawless performance using present communication techniques alone. In conventional UWB localization methods, the system controller uses various localization techniques to estimate the present positions of the users. The accuracy of conventional approaches is dependent on the type of localization algorithm and controller configuration. The indoor positioning accuracy of UWB localization was improved in this work by introducing hybrid algorithms to optimize after TDOA measurements were used.

There is a wide gap between the measured and actual targets due to the limitations of hard equipment and environmental obstacles. This study aims to bridge the gap by enhancing in phases following a communication measure. The distance between the beacon and the target nodes is cur-

rently assumed utilizing TDOA parameters in the localization process. Further, target nodes' 2D and 3D coordinates are calculated using an improved Chan algorithm. After that, the estimated position of target nodes is optimized using ELPSO, BPNN.

II. LITERATURE SURVEY

Using indoor navigation techniques, the major purpose is to locate people or things in indoor environments, viz., public buildings, coal mines, tunnels etc. Creating and maintaining accurate maps is challenging, and there is a lack of technology for localization as well as the calibration of equipment to gather enough measurements samples in real time scenarios. Various infrastructure-dependent and infrastructure-independent approaches to indoor localization currently exist. As an example of current network, Wi-Fi and the Global System for Mobile Communications (GSMC).

Sumitra *et al.* [8] A global positioning system (GPS) is not a frame structure on WSN nodes because of power concerns. Nodes in a network can be located based on radio channel characteristics. The method uses received signal strength (RSS) from dispersed environmental nodes, notably within the building, to determine the location of sensor nodes. In addition, the authors evaluated another weight centre-location-based algorithm (WCL) used. Jain *et al.* [10] A new process of investigating the mechanism by which all sensor nodes in a WLAN network can be located. A new method of investigating the mechanism by which all sensor nodes in a WLAN network can be located. A complete analysis was provided to minimize the collinear issue and localization error, with a shorter path and location time, on numerous localization methodologies and route management mechanisms for the mobile beacon node. Moravek *et al.* [11] specify the correlation between perceived value and place of source data is crucial for location's objectives. Various findings demonstrate that the suggested trajectory has less errors in location than the present trajectory used in the study.

Zwirello *et al.* [13]. In their study, the technology configuration, including the UWB transceiver and time measurement module, a system simulation is used to analyse how this contributed to the rise in the data transfer rate. Simulations and measurements are used to investigate the system's contributing factors of error. In addition, techniques for improving the average accuracy of 9cm are being investigated. Positioning error prediction using scenario geometry is provided along with the positioning method. Finally, an analysis of the data is presented. Hua and Seo [14] The precision of a localization system for blue tooth applications is critical. We've developed a method for selecting the trilateration target inside the hexagonal primary unit distance that maximizes accuracy. However, we found that the approaches suggested here were not sufficient to deliver effective services since they did not give a suitable degree of accuracy. Implementing the current research work resulted in an accuracy of 74% with a 1 m standard deviation. About % of the locations were far from their actual areas. If the machine can anticipate

locations more correctly, the accuracy can increase to 88%. Kawai *et al.* [15] An enhanced Kalman filter-based multi-layer perceptron (MLP) was presented to process BLE RSSI data. Lee *et al.* [16] proposed a new technique where signals at a specific frequency were sent by Waveguide, it included RF and audio signals. Distance and trilateration are determined using the TDOA method, and they concluded that TDOA method is more reliable than other methods like AOA. Sheikh *et al.* [18] proposed a technique called Visible Light Communication (VLC) to determine an object's position with minimum localization error, while a signal flows via an optical channel. Uradzinski *et al.* [19] The balanced K-nearest neighbours method and the Bayesian algorithm have been developed for a novel data filtering solution with an average accuracy of 0.81m or less. Numerous methods are available to determine the target's location depending on the technology utilized, including signal metrics like the received signal intensity indication, channel status information and fingerprinting analysis. Due to its inexpensive cost and absence of extra equipment, RSSI is a widely used technique today.

Wang *et al.* [20] proposed a work to accommodate the skewed Time of Flight (TOF) result, but in a Concurrent Time Difference of Arrival C-TDOA approach, this doesn't work. The approximate TOF anchor estimate is utilized to remove the offset clock in the C-TDOA technique on the other side. Mazraani *et al.* [21] discussed the issue that localization is based on the range. This classifies and matches the most popular range-based optimization strategies so that network designers may select the approaches/algorithms that are appropriate for their applications.

Mekelleche and Haffaf [22]. These methods, on the other hand, are more exact, but they also require more resources. Aruna *et al.* [23] a novel approach that mobile beacon is believed to be transported on an equilateral triangle path, containing signal location information on a regular basis mentioned in the study. Han *et al.* [24] proposed that localization describes a categorization method with levels where localization strategies are characterized as centralized, distributed, or centralized localization algorithms produce superior position estimations than centralized and distributed techniques.

Kulaib *et al.* [25] In addition, it's suggested that a grid scan of the entire sensor field be used for path planning. Classification is dependent on distance between nodes in order to increase the position consistency. Iterative multi lateralization technique and algorithm start conditions are also provided to avoid loss of localization accuracy during the iterative phase, according to the study. Zhang *et al.* [26] suggested a numerous localization technique using the TDOA has provided information for UWB MIMO cognitive radar. If there are many targets, different correlation peaks show the TDAs of those targets. Estimate the mapping link between TDOA's and the relevant objectives. Vandersmissen et.al [27] proposed Chan algorithm and the Taylor algorithm are two regular approaches for solving nonlinear positioning equations for radiolocation in a two-dimensional (2-D) space. As a result, Chan approach has a low computational complexity

and good accuracy in high signal-to-noise ratio (SNR) and Gaussian noise environments improved accuracy of node localization due to algorithm hybridization and discussed various methods for recognizing indoor human activity involved a combination of video-camera and radar sensors combined with a convolutional neural network. Rao *et al.* [28], proposed a novel approach that a resource based RSSI was used to calculate the location estimate, and critical resources had to be eliminated. This was done before any validation sets were extracted from the complete and online training phase. During the experiment, the product performed well. As compiled by Qin and co-authors. Using radio sensors for fingerprint-based device-free Wi-Fi indoor identification that can cope with noisy channel status information is presented. Convolutional neural networks (CNN) and interference auto encoders are used in this system. Cai *et al.* [30] discussed ELPSO, a particle swarm optimization technique, is reported to be composed of three variations of PSO under super optimum control, concluded in this study that particles learn not just from their own experience, but also from that of their neighbors. If you're interested in optimizing indoor localization, anyone may benefit from this unique system of education. For UWB indoor localization, this method is used in both the 2D and 3D versions of the technology. Due to this, both 2D and 3D UWB indoor localization are affected. A well-used benchmark, CEC2005, was utilized to assess ELPSO's performance. Two- and three-dimensional ELPSO variants have been tested for UWB indoor localization and have proven that it outperforms the existing PSO algorithms in most tests it is known that ANN has a similarity with the human neurological system. Samantha *et al.* [31]. As a result, it can learn and adapt, and this capability of ANN has been used in this research. Numerous ANN models have been developed based on the connection of neurons. The multilayer perceptron is supervised trained using the back-propagation network learning algorithm. The maximum data rate Bm of 110 kbps was employed with a length of 1024 symbols.

Gharghan *et al.* [32] Current systems are compared with those that use sensor-based fall detection algorithm (S-BFDA), clustering error using ANN technique, and simulation energy consumption using DDA. NN and DDA beat earlier systems in high accuracy, MAE, and battery life. For fall detection, our results show that we can rely on the proposed system's accuracy, which is roughly 49 cm.

III. PROPOSED METHODOLOGY

As a part of the initial work, distance calculation using TDOA measures have been taken from the literature. Simulation has been carried out for 2D and 3D scenarios with improved Chan algorithm to determine the coordinates of specific nodes. The implemented energy disturbances are cleared by using Kalman filter. Further, two optimization techniques, i.e., ELPSO and BPNN along with least square (LS) & TD (tetrahedron) have been proposed to optimize the calculated target node positions, shown in Fig 1 and Fig 2. Ultra-wideband (UWB) is the most promising indoor location
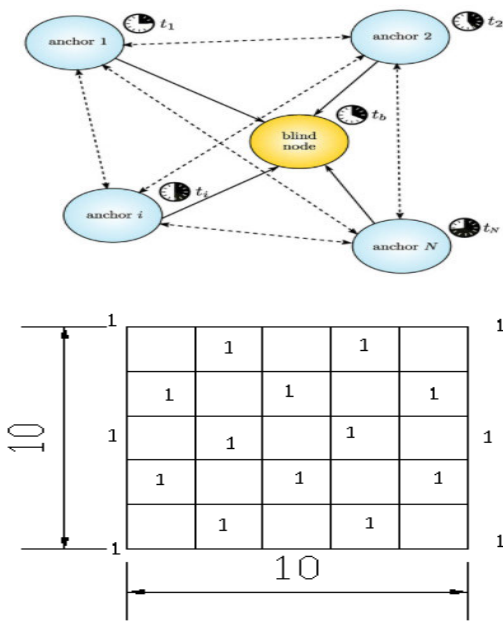
FIGURE 1. (a,b). Anchor node deployment in range-based scenarios using least square method (1 represents the mobile node).

tracking technology among existing wireless technologies. UWB protects against multipath fading. While significant spread spectrum resolvability does not eliminate the negative implications of NLOS and multipath propagating, it does improve. It is easy for NLOS and multipath propagation to cause meters of UWB range error indoors. Indoor location monitoring data can decrease, mainly as a result. An NLOS detection approach using recursive tree structure is proposed provided. UWB channel quality metrics helped us change our model's Gini index and priors splitting criterion.

An Ultra-Wideband-based wireless sensor network communication and location tracking system is the primary objective of this study. Furthermore, system-level evaluation considers objective mobility, functional design, information distribution, and position update delay when assessing distance estimate and tracking approaches. The full 10 m × 10 m top floors of an office building served as a reference environment for the simulations and measurements. Figure 1 shows the location of the beacons in the cabins.

Data from the real world with variable degrees of multipath effects and range errors is necessary to build a good NLOS detection model. LOS and NLOS data sets from the EWINE UWB LOS and NLOS datasets were used in this study to construct the model. UWB channels Cn number 2 with a central frequency of Fc 3.9936 GHz and a bandwidth of B 499.2 MHz were used to collect this data set. As a result, the first-path signal detection average accuracy was improved by preamble lengths of up to 4096.

LIMITATIONS

❖ Wireless Sensor Networks have been investigated utilizing a UWB-based communication and monitoring technology.

❖ Various strategies are presented to deal with latency and resource constraints.

❖ The number of slots utilised to locate a target should be fixed to finalise the target position inside a limited range

A. METHODOLOGY FOR PROPOSED SYSTEM

The relevant distance between the beacon and target node can be calculated through TDOA (Time Difference of Arrival) implementation. The multiple TDOA based positioning system with estimated position is optimized by using the Chan algorithm. The positioning system further checked with Kalman filter. Optimization defines minimizes the variance of the estimation error. PSO is a well-known algorithm for optimization. In this work, the algorithm hybridized with ensemble learning and back propagation of neural networks. Multiple anchors were placed in the selected indoor environment to get high accurate positioning of the moving target node. The Fig 3 depicts the Implementation flow of node localization.

1) TDOA MEASUREMENT

In addition to being more adaptable than ToA, time difference of arrival (TDOA) is the second most commonly utilized range approach. Time of reception and speed are all that are required for this strategy. Neither the target's broadcast time nor the receiver's time of transmission are necessary. Using the difference in arrival times, equation 1 can be used to determine the distance between both variables and the objective.

$$\Delta d = c^* (\Delta t) \tag{1}$$

where c is the speed of light and Δt is the difference in arrival times at each reference point. The distance calculation can be done by equation 2.

$$\Delta d = \sqrt{((X_2 - X)^2 - (Y_2 - Y)^{2-}(X_1 - X)^2 - (Y_1 - Y)^2)} \tag{2}$$

Which corresponds to the known positions of the beacons (X_1, Y_1) and (X_2, Y_2). A hyperbolic equation can be created by converting this equation to a nonlinear regression equation using nonlinear regression.

2) LEAST SQUARE AND METHOD OF ESTIMATION

The 2D objective localization based on TDOA measurement is shown in a non-line of sight condition. Four base stations i.e. BS_1 to BS_4 has been considered as anchor nodes. The source is sending the signal (t) to the nearest BS.

The source is sending the signal (t) to the nearest BS. For i=1,2,3, 4,5 …. N iterations, BS (i) receives the N+1 signal whereas Yi (t) is the time of positioned anchors.
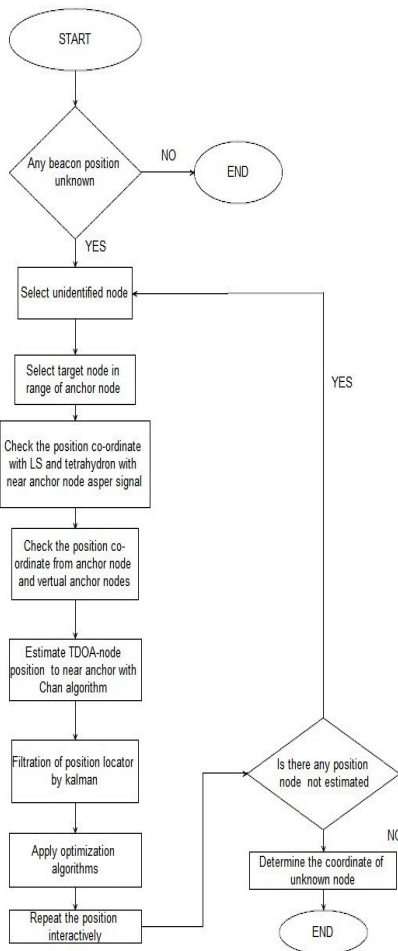
The received signals are given by equation 3

$$yi(t) = ais(t - Ti) + ei(t), \quad i = 1, 2, 3 \dots n \tag{3}$$

an undefined transmitter and unknown receiver, which have their respective positions in space as shown in the Fig below.
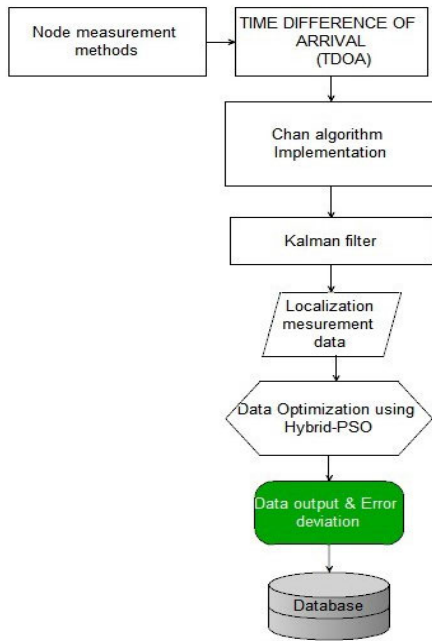
(a)

(b)

FIGURE 2. **(a,b). Implementation flow of node localization.**
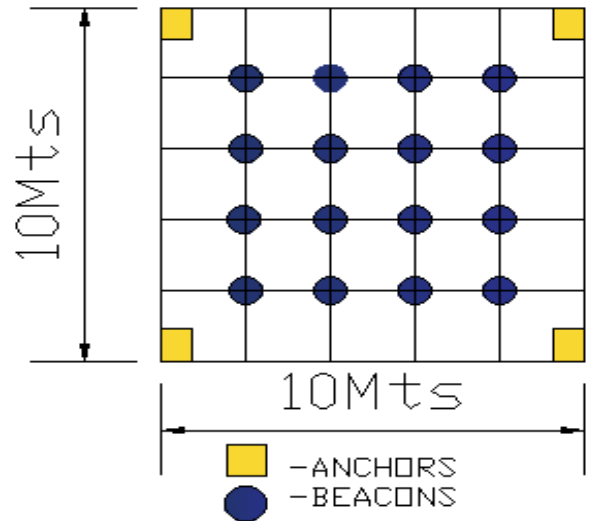

FIGURE 3. Anchor node deployment in range-based scenarios using least square method.

Utilizing the n-least-squares framework with GPS, it is conceivable to estimate the TOA- i and (x, y). When there is no established reference, a pairwise comparison of the received signals can be employed. Using a correlation function, pairwise estimation may be done by the equation 4 where τ is the arrival time coordinate from base station i,j represents distance representatives of x and y axis.

$$\Delta d_{(i,j)} = v(\tau_i - \tau_j), \quad 1 \leq i < j \leq n \tag{4}$$

where v represents the terminal velocity, light, and liquid motions. N in this case stands for the number of receivers, whereas i and j are an enumeration of all K receiver pair configurations, where K is the number of receivers and given by the matrix equation 5.

$$k = \binom{n}{2} \tag{5}$$

A Wave form consists of locations (x, y) along a $\Delta d_{(i,j)}$ line. Start by assuming both of the receivers are in the same line of sight, with their respective positions being equal to d_2. Then Δd can be simplified with the co-ordinate values of x,y, the respective distance value added to x differential as D/2. Therefore, the hyperbolic function can be calculated by using equations 6 and 7.

$$d_2 = \sqrt{y^2 + (x + D/2)^2} \tag{6}$$

$$d_1 = -\sqrt{y^2 + (x - D/2)^2} \tag{7}$$

Then the Δd calculated with the equation 8 where the h differential D also includes

$$\Delta d = d_2 - d_1 = h(x, y, D) \tag{8}$$

By simplifying and rewriting the equation 8 and 9, the average distance value Δd is written by the equation 10.

The hyperbolic function in global coordinates is thus given by $\Delta d_{(i,j)} = h(x, y, D)$ in (8), with differential in diagonal distance can be written using equation 9.

$$D = \sqrt{(Y_i - Y_j)^2 + (X_i - X_j)^2} \qquad (9)$$

$$\Delta d = \sqrt{y^2 + (x + D/2)^2} - \sqrt{y^2 + (x - D/2)^2} \qquad (10)$$

The equation 11 can be written to simplify for hyperbola centroid will be

$$\frac{x^2}{a} - \frac{y^2}{b} = \frac{x^2}{\Delta d^2/4} - \frac{y^2}{\frac{D^2}{4} - \frac{\Delta d^2}{4}} = 1 \qquad (11)$$

Simple translation of the hyperbolic function (5) between local to global coordinates is required for a general receiver position in matrix a simple trigonometric function for x and y coordinates using sin and cos represents for opposite and adjacent coordinate values where α is the angle of moment written in equation 12.

$$\begin{pmatrix} X \\ Y \end{pmatrix} = \begin{pmatrix} X_O \\ Y_O \end{pmatrix} + \begin{pmatrix} Cos(\alpha) & -Sin(\alpha) \\ Sin(\alpha) & Cos(\alpha) \end{pmatrix} \begin{pmatrix} x \\ y \end{pmatrix} \qquad (12)$$

Here, $X0 = (Xi + (Yi + (Xj)/2)/2)/2$ is the center of the receiver pair, while $y0 = (yi + (Yj)/2)/2$ is its equivalent.

There are N (N > 3) sensor nodes, the coordinates of the sensor nodes are known, which are $S_i = (a_i, b_i)^T$, $i \in \{1, 2, \ldots, N\}$, where $[i]^t$ denotes the matrix transpose. It is $p(x, y)^T$ for the target. If the sensor can be attached to two anchors, the formula will be as follows if it doesn't fall within the above-mentioned number of instances. Considering the measuring distances as (a_i, b_i) represents to x and y coordinate with difference matrix (12), the equation can be rewritten as 13,

$$a_i \varphi_i \approx b_i \qquad (13)$$

With the error verification φ_i equation 14 written for the i_{th} coordinate as

$$a_i = \begin{bmatrix} x_{i1} & y_{i1} & 1 \\ x_{i2} & y_{i2} & 1 \end{bmatrix} \qquad (14)$$

From the above matrix, the equation 15 written for b_i for sensor coordinate as

$$b_i = \left(r_{i1}^2 - x_{i1}^2 \right)^2 - y_{i1}^2 + r_{i2}^2 - x_{i2}^2 - y_{i2}^2).^T \qquad (15)$$

The diagonal distance transpose matrix for sensor to node location written in the equation 16 as

$$\varphi_i = \begin{bmatrix} \varphi_i^T & \varphi_i^T & \varphi_i \end{bmatrix}^T. \qquad (16)$$

There are four intersection points with the anchor, least-squares developed with all the near Anchors to check the position where (x_i, y_i) become the least distance. Numeric values can be generated using a basic positioning geometrical technique done using a formula. The line that connects the two locations is originally discovered in this case. When it
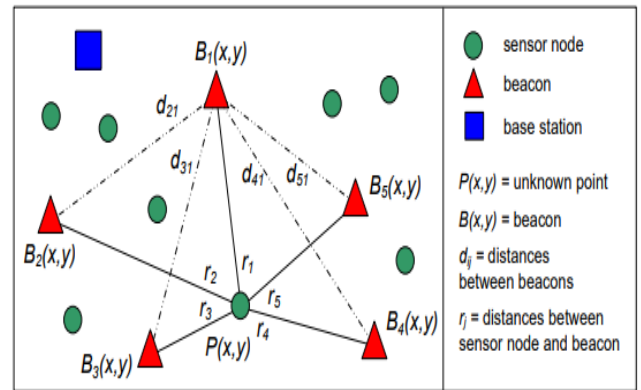

FIGURE 4. Distance calculation between anchor and moving target nodes.

comes to findving the x-coordinate, the equation 17 expressed as

$$x = \frac{-\gamma \pm \sqrt{\gamma^2 - 4a}}{2a}. \qquad (17)$$

Suppose when we have to determine the equation of line of best fit for the given data, the equation of least square line is given by $y = a + bx$, where the equations (18) for a is $\sum y = na + b \sum x$ and for b it is

$$\sum xy = a \sum x + b \sum x^2 \qquad (18)$$

In order to calculate the covariances, sensors need to exchange their current position predictions with those of their neighbors and the distance between them. The sensor that will receive several estimates can be positioned for better combination among that low distance will be considered. Consider the position known as i the values of covariance, and the error can be estimated and positioned as i_1. Among all the error deviations, the slightest error e_1 finalize with the combination and shown as Fig 4.

3) TETRAHEDRON 3D METHOD FOR ESTIMATION

The unknown node receives the signal of all the anchor nodes in the communication range, record their RSSI value, and set up a set of RSSI values in the order from big to small, then take the RSSI value of the larger anchor nodes.

Anchor nodes are selected from the network and then communicated with through radio and unknown nodes to capture the RSSI value. It's possible to create a tetrahedral network by manually selecting a number of anchor nodes that have been received by the reference nodes. As shown in Fig 5, A_1, A_2, A_3, A_4 is the four known-mark of anchor node, it is easy to calculate the distance of A_1, A_2, A_1A_3, A_1A_4, A_2A_3, A_2A_4, A_3A_4. Further the distances, i.e., MA_1, MA_2, MA_3, MA_4 are calculated.

Calculate the volume of A_1, A_2, A_3, A_4, $MA_1A_2A_3$, $MA_1A_2A_4$, $MA_1A_3A_4$, $MA_2A_3A_4$, the volume value V is as V_1, V_2, V_3, V4, respectively. If ($(V_1+V_2+V_3+V_4 > V)$, you can determine the M in the outside of the tetrahedral $A_1A_2A_3A_4$, discard the modified tetrahedral. The average
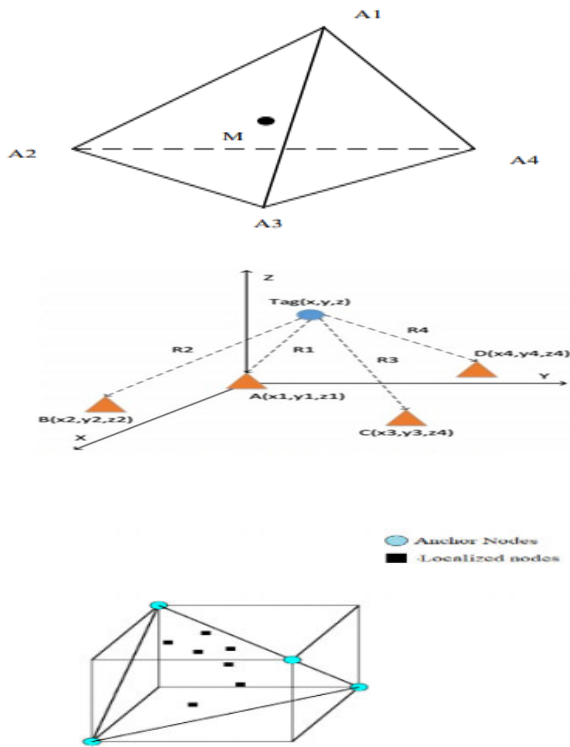
FIGURE 5. Structure of 3D- tetrahedron with- 4 anchor nodes.

distance taken in to consideration where N become number of measurements an R(i) is distance between anchor and target nodes. Finally, the arithmetic mean of the N RSSI values of the unknown node to the same anchor node is considered as the final RSSI value of the anchor node.

The Cartesian coordinates of the four vertices are, (x_1, y_1, z_1), (x_2, y_2, z_2), (x_3, y_3, z_3), (y_4, x_4, z_4), rij is the distance between the vertices I and j. Then the formula for the calculation of its volume is as follows:

$$\text{RSSI} = \sum_{i=1}^{n} R(i)/N \tag{19}$$

Then the calculation of its volume is as derived by the matrix equation (20)

$$V = \frac{1}{6} = \begin{vmatrix} 1 & 1 & 1 & 1 \\ x_1 & x_2 & x_3 & x_4 \\ y_1 & y_2 & y_3 & y_4 \\ z_1 & z_2 & z_3 & z_4 \end{vmatrix}$$

$$= \frac{1}{6} \begin{vmatrix} x_2 - x_1 & y_2 - y_1 & z_2 - z_1 \\ x_3 - x_2 & y_3 - y_2 & z_2 - z_1 \\ x_4 - X_3 & y_4 - y_3 & z_4 - z_3 \end{vmatrix} \tag{20}$$

A set of centroid coordinates then one group per 4, composed of new tetrahedral set, if the group is not divisible by 4, then the rest of the centroid coordinates into the next round of the tetrahedron of reference centroid iteration calculation. We can repeat the above process many times until we get four centroid coordinates to remain. Only two or three centroid

coordinates are remaining. These can be used as the final node estimations. Consider 50 unknown nodes, a communication distance of 10m, and a random pick of 4 anchor nodes consisting of the tetrahedral shape to see if there are any unknown nodes to filter out position errors. The probability of a non-localized node having a nearest neighbor is high, resulting in a high localization ratio.

The localization ratio (LR) is measured by equation 21, where N_l is the number of localized nodes and N_t is the total number of non-localized nodes.

$$\text{LR} = N_l/N_t \tag{21}$$

It's possible to do this by keeping an array next [0. N-1] so that next [p] represents the index of another node within that same tetrahedron (or −1 in case there is no such node). This point is placed in a mesh data structure with the tetrahedron as the first point in the list of points.

The localization error per localized node is calculated by equation 22.

$$L_{\text{error}} = \sum_{i=1}^{Nl} \sqrt{(u_i - x_i)^2 + (v_i - y_i)^2 + (w_i - z_i)^2}/N_L \tag{22}$$

There are NL localized nodes in the network, and their coordinates are (ui, vi, wi) in actual space; however, their estimated co-ordinates (xi, yi, zi) in virtual space. The algorithmic flow of target flow node localization is given in Algorithm1

Algorithm 1 Target Node location
---
1. Input: define objective function (LS/ Tetrahedron)
2. Output: Localization data
3. Initialize: anchor placement-P
4. Number of targeted nodes-N
5. Define localization measured co-ordinates (x_i, y_i) (x_i, y_i, z_i)
6. Activate sensor nodes (anchors)
7. For i= least co-ordinate
8. For anchor $P_i \approx$ check the least value of target
9. If P<Pi, then fix the value.
10. If not repeat steps 5,6,7
11. Run for the least coordinate Pi
12. End if
13. Evaluate
14. Update for measured values
15. End for
16. End.
---

4) IMPLEMENTATION OF CHAN ALGORITHM
The Chan algorithm could attain all TDOA by measuring and obtaining a specific analytical solution; All nonlinear equations are transformed into a set of linear equations before TDOA's known relevant data is used to determine the best condition as soon as this is done, the second phase uses a weighted least squares algorithm to estimate where the

nodes will be measured. In the improvement of the first least-squares calculation of the Chan algorithm, the calculation method of the 2D/3D Chan algorithm is used, and one of the arithmetic formulas and the two matrices are improved. In the original Chan algorithm, only the point coordinates in the area enclosed by each base station can be located, so the utility is not high. In response to this problem, this paper proposes the first least-squares measurement error discriminant method. After the first weighted least squares solution of the Chan algorithm, Δ x, Δ y, and Δ z with positive and negative values are obtained, and the positive and negative values of Δ x, Δ y, and Δ z are obtained according to the first time, respectively. The related correspondence is obtained for the second time. This method makes it possible to locate any mobile terminal within the base station signal coverage.

The distance calculation formula of the base station and the mobile terminal is improved by using the equation 23

$$r_i = \sqrt{(x_i - x)^2 + (y_i - y)^2 + (z_i - H)^2} \qquad (23)$$

H is the height of the mobile terminal measured by the air pressure, and (x_i, y_i, z_i) is the coordinate of the ith base station. Since the TDOA is a 3D value, the height difference obtained by the air pressure measurement is added when calculating the distance. The distance considered as d_i, measurement point is (x, y) and reference base station it is (x_i, y_i), the distance between observed node and the standard base station is then calculated by using the equation 24.

$$\begin{aligned} d_i^2 &= (x_i - x)^2 + (y_i - y)^2 \\ &= K_i - 2x_ix - 2y_iy + x^2 + y^2 \end{aligned} \qquad (24)$$

where, $K_i = x^2 + y^2$, d_{i1} is represents the difference in distance between the label and the ith base station.

When $i = 3$, two measurements can be performed, two equations of two variables can be produced using equation transformation, and the assumed location of the target may be solved.

When $i \geq 4$, let $R^2 = x^2 + y^2$, When the true location of Za0 is determined to be $(x0, y0, R0)$, the error vector (φ) for the variables can be established. There are no known targets in the equation 25, which is written as

$$\varphi = \text{H} - G_a Z_a \qquad (25)$$

where the H becomes the height calculation of the node in 3D space and G_a is the node coordinates the distance matrix written as following equation:

$$H = \begin{pmatrix} d_i^2 - & K_1 \\ d_2^2 & K_2 \\ 3 & . \\ 1 & . \\ 2 & 2 \\ d_n^2 - & K_n \end{pmatrix}, \quad G_a = \begin{pmatrix} -2x_1 & -2y_1 & 1 \\ -2x_2 & -2y_2 & 1 \\ . & . & . \\ . & . & . \\ . & . & . \\ -2x_n & -2y_n & 1 \end{pmatrix},$$

$$Z_a = \begin{pmatrix} x \\ y \\ R \end{pmatrix} \qquad (26)$$

Let the measurement error of each reference node be Iδ, then error value of i_{th} node calculated by using the equation 27.

$$\varphi_i = d_i{}^2 - (d_i{}^0)^2 = (d_i{}^0 + \delta_i)^2 - (d_i{}^0)^2 = 2d_i{}^0\delta_i + \delta_i^2 \qquad (27)$$

The reference node's real value, is represented by $d_i{}^0$. By using the weighted least squares (WLS) method, get an initial estimate of Za. Where the time of arrival expressed as T, for each G_a it can be expressed and the equation 28 written as

$$Z_a = (G_a{}^T\o^{-1}G_a)^{-1}G_a{}^T\o^{-1}H \qquad (28)$$

Instead of 26, the identity matrix can be utilized in the initial estimation because it is unknown. To check the estimated value of Z_a the equation 29 can be simplify to

$$Z_a = (G_a{}^TG_a)^{-1}G_a{}^TH \qquad (29)$$

In this approach, it is now possible to express the link between the estimated and the real value of the object:

$$Z_{a1} = x_0 + e_1$$
$$Z_{a2} = y_0 + e_1$$
$$Z_{a3} = R_0 + e_1$$

where e_1, e_2, e_3 are estimation errors the expression written to error value of the target by using equation 30. Where e_1, e_2, e_3 are estimation errors the expression written to error value of the target by using equation 30.

$$\text{Let } \varphi_1 = 2xe_1 + e_1^2 \approx 2xe_1, \quad \varphi_2 = 2ye_2 + e_2^2 \approx 2ye_2,$$
$$\varphi_3 = e_3.. \qquad (30)$$

then for N number of node error deviation finalized and rewritten in equation 31:

$$\varphi' = \text{H}'^- G_a' Z_P \qquad (31)$$

The transpose matrix with time differential error vector Z_p written for equation 32

$$\text{where,} \quad H^1 = \begin{pmatrix} \hat{Z}_{a1}^2 \\ \hat{Z}_{a2}^2 \\ \hat{Z}_{a3}^2 \end{pmatrix}, \quad G_{a^1} = \begin{pmatrix} 1 & 0 \\ 0 & 1 \\ 1 & 1 \end{pmatrix},$$

$$Z_p = \begin{pmatrix} x^2 \\ y^2 \end{pmatrix}, \quad \varphi^1 = [\varphi_1', \varphi_2', \varphi_3']^T \qquad (32)$$

$\text{T } \varphi^I = \varphi^1\varphi^2\varphi^3$ is the error vector of Z_p. The estimated value of Z_p is calculated using the equation 33 as improvement.

$$Z_p = (Ga'^T\o'^{-1}Ga')^{-1}Ga'^T\o'^{-1}H' \qquad (33)$$

The location result obtained by the two WLS calculation referred to the equation 34:

$$Z = \pm\sqrt{Z_p} \qquad (34)$$

There should be no difference in the sign of the selected (x, y, z) in Zp and in the Zp selected inside the placement region as a solution to a problem.

Filtration: Kalman filtering is a two-stage process that begins with prediction and ends with upgradation Variables

will be estimated during the prediction process. On the other hand, the update step involves updating information based on current situations. The Kalman filter's process is as follows.

In order to determine the mobile node's range signal, N beacon nodes are placed in the field at various times. For example, if you want to know where the nth beacon node is, you need to know (X_n, Y_n), where $n = 1, \ldots, N$. In a 2D-plane, the mobile node moves randomly, with state vector $x(k) = [x(k)\ y(k)]$. A mobile node's position and velocity can be described by the expression T at each time step of time step, where time step k is equal to 1, 2, 3, 4, etc. As a result of the change in x(k) at iteration interval. A beacon node's (xm, ym) coordinates are $(m = 1), \ldots, (m = M)$, where M is the number of beacon nodes in the network. With state vector x(k), the mobile node moves randomly in a 2-dimensional plane. A mobile node's position and velocity can be expressed as (x(k)/y (x(k)) at each time step, $k = 1, \ldots, K$. According to equation 35, X(k) changes at time step k to describe its movement.

$$k, \hat{x}_k = F_k x_{k-1} + B_k u_k \tag{35}$$

where In this example, the correlation coefficient l (T, H) is the correlation coefficient between the temperature of the ith hour (ti) and humidity (hi) of the ith hour (ti). T and H represent the arithmetic mean of humidity levels, respectively. The position of the node represented by using the equation 36. where P_k is the post estimate error covariance and the filtration can be written in the equation 37. Filtering the temperature and humidity along x vector the equation written as 38 where H relates the state X_k to the measurement Z_k

$$P_k = F_k P_{k-1} F_k^T + Q_k \tag{36}$$

$$K' = \frac{P_k H_k^T}{H_k P_k H_k^T + R_k} \tag{37}$$

$$x_k = \hat{x}_k + K' \left(z_k - H_k \hat{x}_k \right) \tag{38}$$

The position node can calculate after filtration by using the simplified equation 39

$$P_k = P_k \left(1 - K' H_k \right) \tag{39}$$

Accuracy checked with TP as temperature at node with TN number of nodes in with filtered value and filtered nodes can be calculated using the equation 40 and precision, re verification with the equations 41 and 42. The algorithmic flow of localization with filtration is given in Algorithm 2.

$$\text{Accuracy}: \quad \frac{TP + TN}{TP + TN + FP + FN} \tag{40}$$

$$\text{Precision}: \quad \frac{TP}{TP + TN} \tag{41}$$

$$\text{Recall}: \quad \frac{TP}{TP + FN} \tag{42}$$

$$IoU = \frac{X \cap Y}{X \cup Y} \tag{43}$$

Algorithm 2 Localization With Filtration

1. Input: Measured target co-ordinate
2. Output: Measured data deviation
3. Initialize: Update anchor node list, Checking Pi, transmission

   1(a). Checking the node ID

4. Sending feedback signals 3. Establishing relevant matrices

   3(a). Establishing the estimation matrix
   3(b). Establishing the distance matrix

5. Constructing the approximation matrix
6. Repeating the preceding steps until all matrices are formed

Output Position of the non-anchor node
(1. Picking up the hop range from the anchor node list
2. Calculating the final distance matrix via Ls = Tsp.
3. Positioning the transmission node.
4. Filtration)

7. Return the position information of the target sensor node as the outcome
8. end if
9. evaluate the position
10. update best position Pi
11. end for.
12. End.

IV. OPTIMIZATION WITH ELPSO

Improved PSO has been implemented in the place of traditional PSO with Ensemble learning, the re calculation of measurement for node localization shown in figure-6.

The Basic PSO method consists of a population of randomly distributed particles inside the parameter space. Particles in the parameter space reflect alternative solutions to the design optimization problem because of their positioning. As each particle goes across parameter space, it has a velocity. Some of the advantages of the PSO approach include fewer parameters, faster convergence, and low requirement for gradient information. As part of the algorithm 3, the mass-less particle swarm is used to find the optimal location.

The improved PSO algorithm employs a set of feasible solutions within the search space, called a swarm of particles with random initial locations. Our proposed algorithm reduced the initial search space by using a bounding box method.

In addition, thousands of iterations require massive energy consumption, which will significantly shorten the service period of sensor nodes. In summary, because of the shortcomings of the above localization algorithms, a two-stage PSO algorithm for wireless sensor node localization in the concave region is proposed in this paper. The first stage: based on the similar path and intersecting ratio to determine whether the shortest path between nodes is affected by the concave boundary, then calculate the distances between target unknown nodes and beacon nodes, finally, using the least

Algorithm 3 Optimization Using PSO

1. %% Output: the initial calculated value of the target position (x,y,z)
2. For $1 \leq i \leq N$ Do %% i is each particle
3. Initialization of particles
4. End
5. Do
6. For $1 \leq i \leq N$ Do
7. If fitness (X_i) > p-best i Then p-best-i = X_i;
8. End
9. If %%p-best-i is the best position of $^{i-th}$ particle
10. End
11. For g-besti = opti{p best$_i$i$_1$ $\leq$ i $\leq$ N}%% optimum value
12. For $1 \leq i \leq N$ Do
13. If fitness (X_i) > p-best i Then p-best-i = X_i;
14. Update particle velocity and position according to the equation-9
15. If pbest i > gbest i
16. Then g best i = p best i;
17. End if
18. End for
19. End.

PSO Implementation

1.While (not timeout) {
2. Listen for and collect anchor nodes' information
3. if (discover 3 or more anchor nodes in its neighborhood) {//**MODE 1**
4.CALL procedure **LOCALIZATION**
5. }
6.}
7 //**MODE 2**
8. Get original anchor nodes' information from the packet broadcast by the closest neighbor anchors
9. if (discover 3 or more anchor nodes) {
10. CALL procedure **LOCALIZATION**
11.} else {
12. Set as an orphan node
13.}
14.
15 Procedure **LOCALIZATION**
16. {
17. Use PSO to estimate the location and become an updated anchor node
18. Broadcast the estimated location and the location data of original anchor nodes
19. Localization complete and exit
20. }

square method to complete nodes localization. The second stage uses the improved PSO method to optimize the coordinates calculated in the previous step.
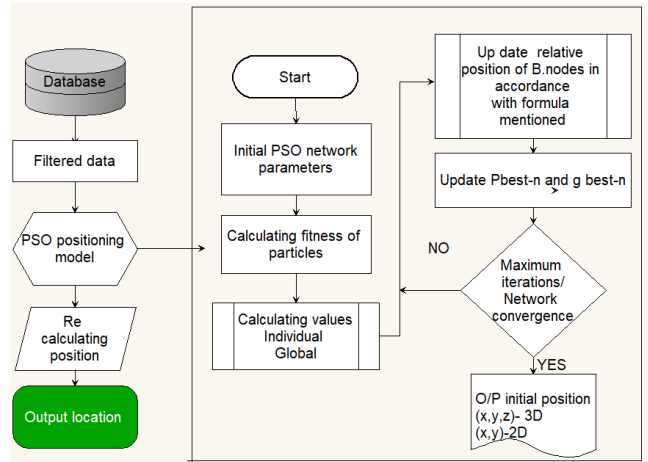

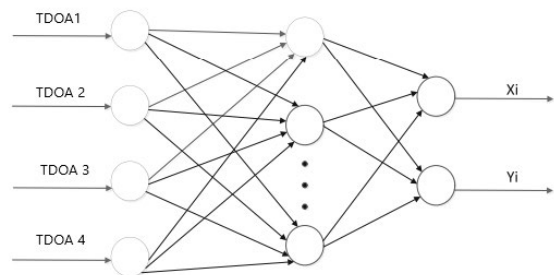**FIGURE 6.** ELPSO based optimization with TDOA node localization 2D & 3D.

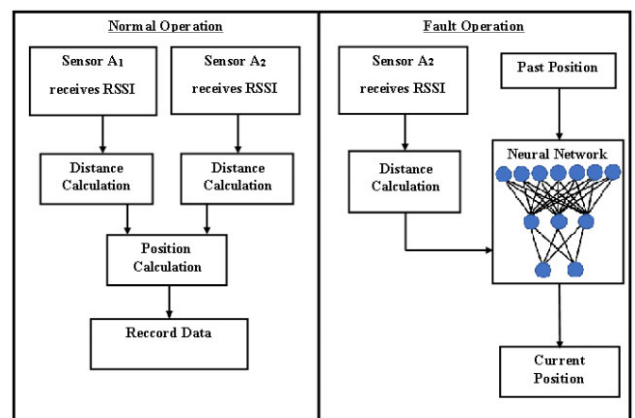**FIGURE 7.** Network process of TDOA in BPNN for real optimal values.

FIGURE 8. Optimal path flow chart by using BPNN.

The present work uses the PSO algorithm in the second stage to inter-relatively optimize the results obtained in the first stage. The aim is to decrease the impact of distance error on the results and improve localization accuracy. The location of beacon nodes are: $a_1(x_1, y_1) \cdots a_i(x_i, y_i) \cdots an(x_n, y_n)$, According to the first-stage ranging algorithm, the distances from beacon nodes to u are: $d_{1u} \cdots d_{iu} \cdots d_{nu}$.

Network Model	Number of Training Data Points	RMSE
BPNN	100	0.1040 m
	256	0.0978 m
	361	0.0350 m
With PSO BPNN	100	0.1820 m
	256	0.0732 m
	361	0.0137 m
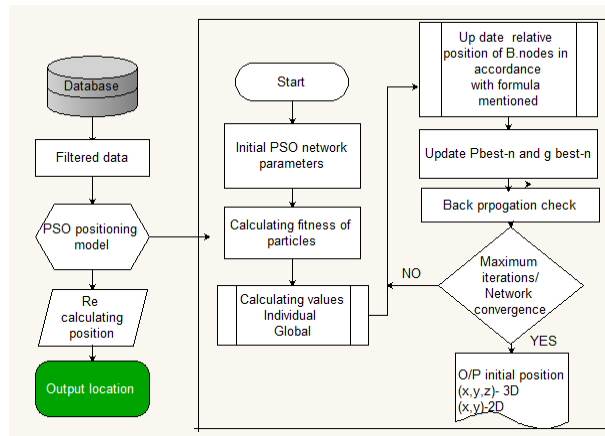
FIGURE 9. Flow chart for BPNN- PSO implementation for optimal error variance.

FIGURE 10. Localization pattern from anchor to dynamic nodes in Indoor network in 3D environment.
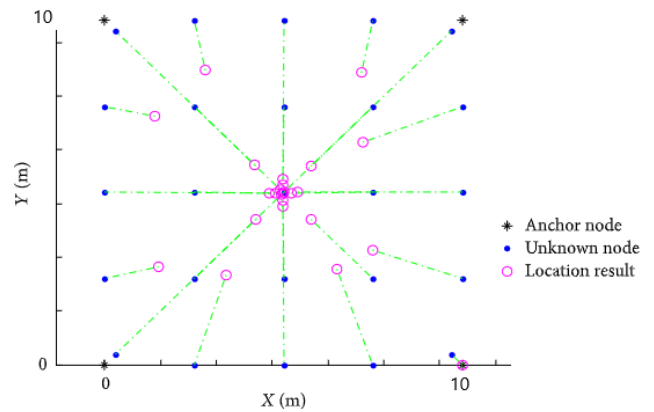
FIGURE 11. Regular deployment of nodes localization.

Assuming m particles are searching for the best solution in D-dimensional space using PSO, the location of the ith particle in the swarm is determined as $X_i = (X_{i1}, Z_{i2}, \cdots \cdots X_{iD})$. The correctness of the particle's positions is evaluated using the objective function at each possible location.

The optimal location that the particle passed is: $Pbest(i) = (P_{i1}, P_{i2}, \cdots \cdots P_{iD})$, record the optimal coordinate currently searched in the entire particle swarm as: $Gbest = (P_{g1}, P_{g2}, \cdots \cdots P_{gD})$.

A. OPTIMIZATION USING ELPSO

To improve the generalization of a single learner's learning, ensemble methods integrate a large number of individual learners. Subsets of original dataset are substituted by random sampling to create subsets, and then individuals are trained on these subsets before integrating them via a vote mechanism. The Fig 6 shows the ELPSO based optimization with TDOA node localization 2D & 3D.

There are two ways in which you can represent particle i's position in N-dimensional space: by using the vectors $[X_{i1}]$ and $[X_{i2}]$ and by using vectors $Vi = [V_{i1}, V_{i2}, V_{i3}, V_{i4}]$. The evaluation function and the particle's personal best position (p_{best}) and current location (X_i) provide each particle a fitness value based on its experience. We also kept track of the best position (g_{best}) for each particle, which is based on
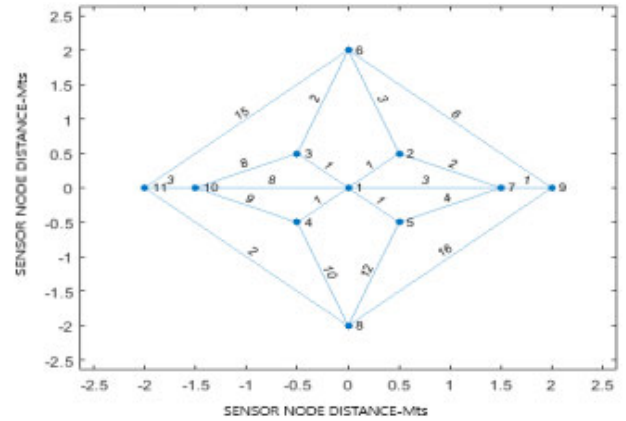
other peers' experiences. By using its own or other particles' best experience to calculate its future movement, the particle updates the corresponding velocity and location. Pbest is the nearest best position Pbest value that classifies the data as a result of the optimized technique. The relative majority voting method is a frequent strategy for classifier combination in algorithms. The prediction output of ensemble learning H1(x) can be obtained as follows: where i, j refers to the position co-ordinates of best X.

$$H_1(x) = C \underset{J}{\underset{argmax}{}} \Sigma_i^L = 1 h_i^j(x) \qquad (44)$$

After the classification of N no. of data points set in particle swam, the recalculated position of P was verified for the lowest nearby value of P (X_i, Y_i). N particles are all included in this space following a distance L from each particle to each base station, and given the observed distance R from target to target for the ith particle and j^{th} target, we get the following

TABLE 1. Co-ordinate values of localization of 2D positioning.

TABLE 1. *(Continued.)* Co-ordinate values of localization of 2D positioning.

Target	Target position (m)	Measured position (m)	Measured error (cm)	Optimized position (m)	Error after Optimization (cm)
1	(-4.50, -4.50)	(-4.86, -4.58)	3.664	(-4.470, -4.462)	3.964
2	(-4.50, -3.50)	(-4.96, -3.24)	5.28	(-4.462, -3.471)	3.762
3	(-4.50, -2.50)	(-4.62, -2.84)	2.36	(-4.472, -2.481)	2.864
4	(-4.50, -1.50)	(-4.31, -1.62)	2.04	(-4.662, -1.534)	3.212
5	(-4.50, -0.50)	(-4.16, -0.82)	4.62	(-4.528, -0.504)	0.3164
6	(4.50, 4.50)	(4.96, 4.38)	4.744	(4.474, 4.530)	2.862
7	(4.50, 3.50)	(4.82, 3.64)	3.396	(4.51, 3.489)	0.3244
8	(4.50, 2.50)	(4.32, 3.10)	4.324	(4.62, 2.536)	3.784
9	(4.50, 1.50)	(4.51, 1.72)	0.584	(4.46, 1.471)	0.3564
10	(4.50, 0.50)	(4.16, 0.82)	4.424	(4.462, 0.535)	0.3458
11	(-3.50, -4.50)	(-3.70, -4.58)	2.064	(-3.533, -4.468)	3.246
12	(-3.50, -3.50)	(-3.92, -3.24)	4.876	(-3.465, -3.535)	3.524
13	(-3.50, -2.50)	(-4.12, -2.84)	7.356	(-3.462, -2.54)	3.824
14	(-3.50, -1.50)	(-3.10, -1.62)	2.8	(-3.529, -1.536)	3.2462
15	(-3.50, -0.50)	(-3.20, -0.82)	4.1	(-3.539, -0.571)	3.662
16	(3.50, 4.50)	(4.16, 4.82)	4.356	(3.458, 4.536)	3.9432
17	(3.50, 3.50)	(3.80, -4.18)	5.4	(3.536, 3.474)	3.2412
18	(3.50, 2.50)	(3.92, -2.64)	4.32	(3.534, 2.478)	2.8214
19	(3.50, 1.50)	(4.12, -1.24)	4.86	(3.471, 1.536)	3.1242
20	(3.50, 0.50)	(3.10, -0.42)	4.32	(3.466, 0.537)	3.4246
21	(-2.50, -4.50)	(-2.60, -4.58)	4.18	(-2.541, -4.529)	3.0816
22	(-2.50, -3.50)	(-1.92, -3.24)	5.46	(-2.465, -3.533)	3.5642
23	(-2.50, -2.50)	(-2.12, -2.84)	7.25	(-2.540, -2.531)	3.8946
24	(-2.50, -1.50)	(-2.90, -1.62)	6.87	(-2.456, -1.537)	3.6343
25	(-2.50, -0.50)	(-3.20, -0.82)	5.64	(-2.54, -0.471)	3.5421
26	(2.50, 4.50)	(2.16, 4.82)	6.28	(2.532, 4.539)	3.7825
27	(2.50, 3.50)	(1.80, 4.18)	6.41	(2.539, 3.458)	3.6462
28	(2.50, 2.50)	(2.92, 2.64)	6.639	(2.460, 2.532)	3.8716
29	(2.50, 1.50)	(2.12, 1.24)	4.620	(2.53, 1.466)	2.9645
30	(2.50, 0.50)	(3.10, 0.42)	4.822	(2.522, 0.474)	2.8654
31	(-1.50, -4.50)	(-1.70, -4.58)	5.367	(-1.541, -4.682)	3.2416
32	(-1.50, -3.50)	(-0.92, -3.24)	3.125	(-1.465, -3.537)	0.3564
33	(-1.50, -2.50)	(-1.12, -2.84)	4.623	(-1.472, -2.534)	3.3230
34	(-1.50, -1.50)	(-2.10, -1.62)	4.821	(-1.529, -1.536)	3.2464
35	(-1.50, -0.50)	(-1.20, -0.82)	4.129	(-1.472, -0.531)	2.9815
36	(1.50, 4.50)	(1.16, 4.82)	3.424	(1.534, 4.699)	2.8242
37	(1.50, 3.50)	(1.80, -4.18)	37.624	(1.465, 3.538)	3.6587
38	(1.50, 2.50)	(1.92, -2.64)	34.396	(1.54, 2.458)	3.9874
39	(1.50, 1.50)	(1.12, -1.24)	4.044	(1.535, 1.532)	3.4824
40	(1.50, 0.50)	(1.10, -0.42)	4.064	(1.47, 0.531)	2.9108
41	(-0.50, -4.50)	(-0.70, -4.58)	2.064	(-1.532, -4.463)	3.1253
42	(-0.50, -3.50)	(-0.92, -3.24)	4.364	(-1.459, -3.538)	3.7846
43	(-0.50, -2.50)	(-0.52, -2.84)	3.404	(-1.54, -2.462)	3.6422
44	(-0.50, -1.50)	(-1.10, -1.62)	6.144	(-1.47, -1.473)	3.2654
45	(-0.50, -0.50)	(-0.70, -0.82)	3.024	(-1.532, -0.469)	2.9321
46	(0.50, 4.50)	(1.16, 4.82)	7.624	(1.469, 4.532)	3.1258
47	(0.50, 3.50)	(1.40, 4.18)	13.624	(1.537, 3.529)	3.6547
48	(0.50, 2.50)	(0.92, -2.64)	4.396	(1.46, 2.54)	3.7624
49	(0.50, 1.50)	(0.62, -1.24)	1.876	(1.541, 1.536)	3.5212
50	(0.50, 0.50)	(1.20, -0.42)	12.9	(1.466, 0.532)	3.4632

Note: m -meters cm- centimeters

fitness function:

$$f(p_i) = (L_A^i - R_A^i)^2 + (L_B^i - R_B^i)^2 + (L_C^i - R_C^i)^2 + (L_D^i - R_D^i)^2 \quad (45)$$

When f = 0, Pi achieved the optimal solution, i.e., Pi exactly located in the position of target.

To find the mean and standard deviation of the solutions in the appendices. When f3, f5, f6, f7, f8 and f13 are considered, the ELPSO achieves the best possible solution in these functions.

B. BPNN-PSO OPTIMIZATION

As a result, classification is one of the most significant Neural Network applications. Many hours are required to solve classification issues, as well as extensive research on all the static patterns that may be used for classes. Hence, the initialization of the swarm (neuron) is done by assigning it to any random place and velocity, as well as the potential solutions that are flown via hyperspace and it is depicted by Fig 7. Neuronal networks are split into two modules in order to achieve high accuracy using TDOA estimate propagation.

Input layer: majority are used in the training set and 20 percent in the test set for each model's input values.

Hidden layer: The number of nodes in a neural network affects its performance on the hidden layer. More complex a network's architecture, the more accurate its output will be, in general. The number of neurons in this research is 8 because of the training time and accuracy of the compromise approach. The Tan(h)-Sigmoid activation function is used to approach any non-linear precision function.

The output layer is composed of two places estimated minimum for 2D and four positions estimated minimum for 3D estimations, respectively and is shown in Fig 8 and Fig 9. Train BP neural network using anticipated values and its actual position first, and then build a group of the new position of unknown node to simulate.

For example, CM_1 symbolizes line-of-sight residential areas, while CM_2 denotes environments that do not have line-of-sight access. RMSE performance of the BP neural network in CM_1 and CM_2 channels can be optimized by hybridizing with PSO by using all of the SNR values.

Sample datasets of 300 were considered out of it 17% of tested samples taken for the optimization of measuring values considered to neurons in error prediction.

These are divided into two sets of 10 each for training and validation. The investigation looks at three training scenarios:

1. Training measurements are collected in all reference locations, and one model per anchor is learned (A=0).
2. Training measurements are collected in all reference locations (M=0), and a single model is learned and applied to all anchors (A=1).
3. Training measurements are collected in every second reference location, and separate models for each anchor is learned (A=0).

Step-1: This neural network functions as a virtual sensor to simulate the information retrieved by a faulty sensor A1 during its failure considering its past data and current information from sensor A2. The neural network is trained with the same inputs as those that it needs for operating. The neural
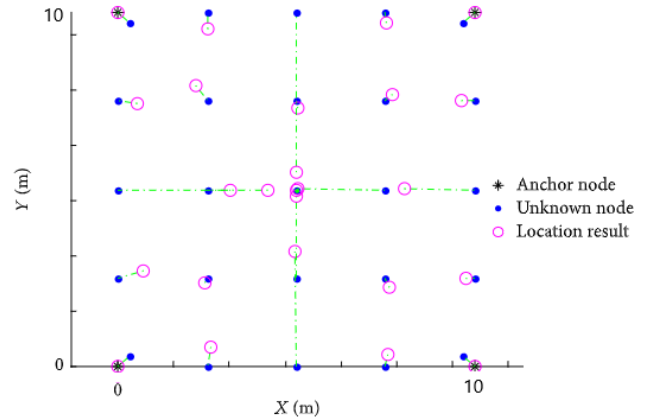

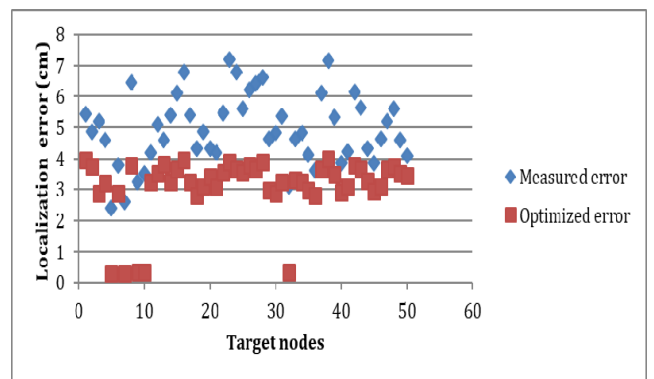**FIGURE 12.** Least square deployment of nodes localization.

FIGURE 13. Comparison of measured localization error with optimized error in 2D scenario.
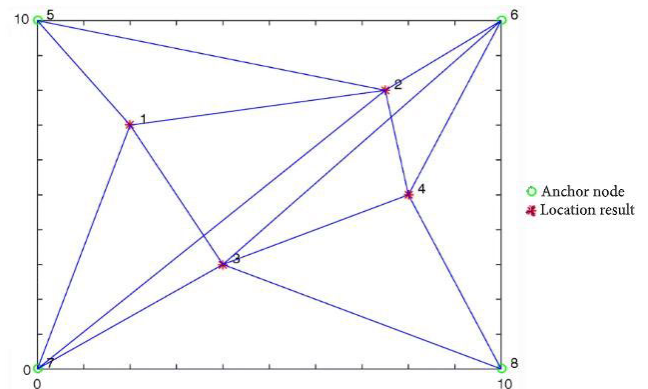

FIGURE 14. Error fitness deviation after repeatable test with dynamic nodes.

network comprises an input layer, at least one inner layer (also called a hidden layer), and one output layer. The input layer receives the data and introduces them to the other neurons. In this study case, the input layer needed four neurons to work correctly, as there were four inputs besides the bias, which was considered to have the value of 1. Thus, this neural network received past positions $(x(t-1), y(t-1)), (x(t-2),$
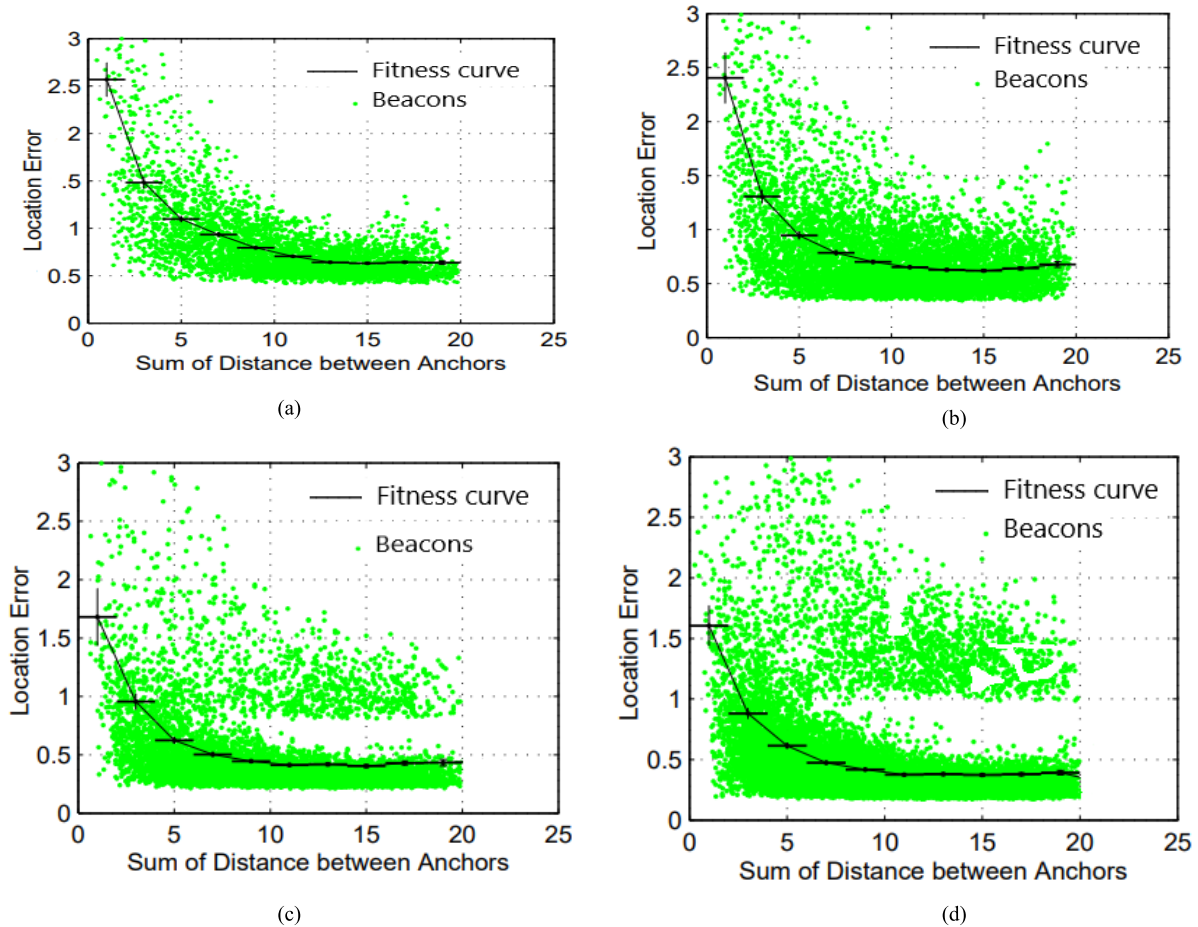
FIGURE 15. Comparative analysis of various algorithms at various positions. (a) Fitness graph of beacon measurement at position 1. (b) Fitness graph of beacon measurement at position 2. (c) Fitness graph of beacon measurement at position 3. (d) Fitness graph of beacon measurement at position 4.
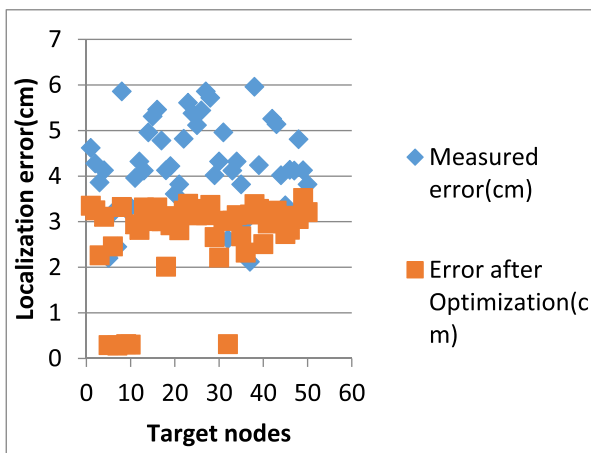

FIGURE 16. Error fitness deviation after repeatable test with dynamic nodes.

$y(t-2))$, current and past distances calculated from sensor $A2(r(t),r(t-1),r(t-2))$.

Step-2: The output layer consisted of two neurons that provide the estimations of the node's position. Comparing the last two positions allows the machine-learning algorithm

to estimate the movement's speed and inertial tendency. The outputs of the algorithm are coordinates in the X and Y axes for each interaction step. The figure shows this neural network.

Step-3: Time-series correlations were performed to evaluate the linear temporal relationships between X and Y coordinates, the past time values of these variables, and the measured distances of sensor r2. The steps were each of the last discrete positions measured for each variable. The time from one stage to another varied according to the individual speed of the target.

Step-4: Comparing the mean error with the median reveals that the statistical distribution of errors presents symmetrical behaviour, maybe with a very short tail to the left, similar to the behaviour of the X-axis.

Step-5: The virtual sensor could replace the actual sensor for some time, provided that the past position/trajectory was known and the calculated position is within the active sensor radius. This replacement would work even if the original sensor was already at a greater distance than the one considered between the sensor nodes of the experiments performed in this work, and one failed. From one

TABLE 2. Co-ordinate values of localization of 3D positioning.

Target	Target position (m)	Measured position (m)	Measured error (cm)	Optimized position(m)	Error after Optimization(cm)
1	(-4.50,-4.50,4.8)	(-4.86,-4.58,4.2)	7.264	(-4.832,4.541,4.762)	3.351
2	(-4.50,-3.50,4.6)	(-4.96,-3.24,4.6)	4.716	(-4.924,3.468,4.631)	3.252
3	(-4.50,-2.50,4.4)	(-4.62,-2.84,3.9)	4.856	(-4.581,2.486,4.343)	2.264
4	(-4.50,-1.50,4.2)	(-4.31,-1.62,4.4)	1.961	(-4.532,1.472,4.241)	3.112
5	(-4.50,-0.50,4.0)	(-4.16,-0.82,3.6)	6.024	(-4.522,-0.552,3.94)	0.2964
6	(4.50,4.50,3.8)	(4.96,4.38,3.5)	5.64	(4.978,4.42,3.714)	2.462
7	(4.50,3.50, 3.6)	(4.82,3.64,3.8)	3.8	(4.534,3.582, 3.628)	0.2844
8	(4.50,2.50,3.4)	(4.32,2.10,3.2)	3.8	(4.451,2.403,3.434)	3.324
9	(4.50,1.50,3.2)	(4.51,1.72,3.1)	1.485	(4.515,1.478,3.204)	0.3164
10	(4.50,0.50,3.0)	(4.16,0.82,2.9)	4.524	(4.298,0.503,2.994)	0.3058
11	(-3.50,-4.50,2.8)	(-3.70,-4.58,2.6)	3.906	(-3.544,-4.538,2.76)	2.946
12	(-3.50,-3.50,2.6)	(-3.92,-3.24,2.5)	4.32	(-3.534,3.443,2.562)	2.824
13	(-3.50,-2.50,2.4)	(-3.32,-2.84,2.3)	4.112	(-3.458,2.572,2.364)	3.314
14	(-3.50,-1.50,2.2)	(-3.20,-1.62,2.1)	4.936	(-3.417,1.546,2.231)	3.0162
15	(-3.50,-0.50,2.0)	(-3.28,-0.82,1.95)	5.341	(-3.419,0.614,2.033)	3.222
16	(3.50,4.50,1.8)	(3.36,4.82,1.87)	5.468	(3.444,4.592,1.832)	3.3132
17	(3.50,3.50,1.6)	(3.80,3.18,1.52)	4.781	(3.572,3.454,1.634)	3.0112
18	(3.50,2.50,1.4)	(3.72,2.64,1.3)	4.13	(3.565,2.545,1.36)	2.014
19	(3.50,1.50,1.2)	(3.12,1.24,1.15)	4.22	(3.434,1.457,1.171)	2.9242
20	(3.50,0.50,1.0)	(3.10,0.42,1.08)	3.61	(3.419,0.436,1.044)	3.1246
21	(-2.50,-4.50,0.8)	(-2.60,-4.58,0.9)	3.828	(-2.541,-4.53,0.825)	2.816
22	(-2.50,-3.50,0.6)	(-1.92,-3.24,0.75)	4.824	(-2.389,-3.44,0.643)	3.2442
23	(-2.50,-2.50,0.4)	(-2.12,-2.84,0.58)	5.61	(-2.38,-2.564,0.483)	3.3946
24	(-2.50,-1.50,0.2)	(-2.90,-1.62,0.3)	5.388	(-2.594,1.541,0.232)	3.2343
25	(-2.50,-0.50,0.0)	(-2.20,-0.82,0.15)	5.12	(-2.442,-0.571,0.04)	3.1421
26	(2.50,4.50,4.8)	(2.16,4.82,4.2)	5.44	(2.398,4.545,4.832)	3.2825
27	(2.50,3.50,4.6)	(2.80,3.18,4.6)	5.860	(2.584,3.434,4.633)	3.1462
28	(2.50,2.50,4.4)	(2.92,2.64,3.9)	5.726	(2.592,2.567,4.366)	3.3716
29	(2.50,1.50,4.2)	(2.12,1.24,4.4)	4.027	(2.396,1.412,4.228)	2.6645
30	(2.50,0.50,4.0)	(2.10,0.42,3.6)	4.323	(2.422,0.477,3.981)	2.2154
31	(-1.50,-4.50,3.8)	(-1.70,-4.58,3.5)	4.969	(-1.582,4.534,3.764)	3.0216
32	(-1.50,-3.50,3.6)	(-0.92,-3.24,3.8)	2.624	(-1.299,3.464,3.638)	0.3164
33	(-1.50,-2.50,3.4)	(-1.12,-2.84,3.2)	4.121	(-1.413,2.548,3.364)	3.0230
34	(-1.50,-1.50,3.2)	(-1.10,-1.62,3.1)	4.320	(-1.426,1.545,3.162)	3.1464
35	(-1.50,-0.50,3.0)	(-1.20,-0.82,2.9)	3.824	(-1.399,0.564,2.962)	2.6815
36	(1.50,4.50,2.8)	(1.16,4.82,2.6)	3.027	(1.434,4.452,2.763)	2.3242
37	(1.50,3.50,2.6)	(1.80,3.18,2.5)	2.122	(1.566,3.432,2.568)	3.1587
38	(1.50,2.	(1.72,	5.96	(1.581,2.5	3.3874

TABLE 2. *(Continued.)* Co-ordinate values of localization of 3D positioning.

TABLE 2. *(Continued.)* Co-ordinate values of localization of 3D positioning.

	50,2.4)	2.64,2.3)	9	54,2.359)	
39	(1.50,1.50,2.2)	(1.12,1.24,2.1)	4.241	(1.421,1.461,2.168)	3.2824
40	(1.50,0.50,2.0)	(1.10,0.42,1.95)	4.089	(1.399,0.459,1.972)	2.5108
41	(-0.50,-4.50,1.8)	(-0.70,-4.58,1.87)	2.113	(-0.545,4.534,1.845)	2.9625
42	(-0.50,-3.50,1.6)	(-0.62,-3.24,1.52)	1.94	(-0.541,-3.459,1.56)	3.1846
43	(-0.50,-2.50,1.4)	(-0.52,-2.84,1.3)	3.504	(-0.538,2.563,1.366)	3.2422
44	(-0.50,-1.50,1.2)	(-1.10,-1.62,1.15)	6.169	(-0.942,1.553,1.162)	3.0654
45	(-0.50,-0.50,1.0)	(-0.70,-0.82,1.08)	3.088	(-0.544,-0.538,1.032)	2.7321
46	(0.50,4.50,0.8)	(1.06,4.82,0.9)	6.724	(0.884,4.542,0.832)	2.8254
47	(0.50,3.50,0.6)	(0.40,4.180,0.75)	6.224	(0.462,3.988,0.633)	3.1324
48	(0.50,2.50,0.4)	(0.72,2.64,0.58)	2.72	(0.682,2.541,0.431)	3.0622
49	(0.50,1.50,0.2)	(0.62,1.24,0.3)	2.844	(0.539,1.465,0.239)	3.5212
50	(0.50,0.50,0.0)	(1.20,0.42,0.15)	5.925	(1.094,0.468,0.094)	3.2132

Note: m -meters cm- centimeters

sensor with the corresponding measured position of the other sensor through MATLAB function corr() that establishes the pairwise correlation coefficient between each pair of vectors, which comprised the time series of the positions detected by each sensor. This correlation was found by comparing the registered data for each of the measured positions.

Back Propagation Neural Network Model with 20 neurons in the hidden layer was trained with 100 data points' dataset. This network was tested with the test data set, from where a root mean square error of 0.1040 m was calculated. After that this network was trained with 300 data points' dataset. This was again tested with the same dataset, now it gave a root mean square error of 0.0350 m. The actual position and the estimated position of each node after simulation for both the

cases (100 data points training and 300 data points training). Next a radial Basis Function network model with 100 neurons in the hidden layer was trained with the same 100 data points' dataset and after testing it with the test dataset.

A framework for detecting external objects in a UWB sensor network was developed using the BPNN method. Fig. 9 The performance of the localization approach compared with the least-squares estimator. Backward error propagation and weight correction. Neuron error gradients are computed in the output layer:

A steady result is the objective of previous neural networks (e.g., the Multilayer Perception) P(d|x), a pdf of the inter-node distance conditioned on the pre-processed feature vector, has been extended from the traditional neural network technique. $\vec{x} = (x_1, \dots\dots\dots\dots\dots\dots\dots\dots, x_n)^T$ $[1, \dots, x^\sim M]^T$ to get better output data.

$$x_m = -1 + \frac{2(x_m - x_{m,min})}{x_{m,max} - x_{m,min}} \quad m = 1, \dots\dots\dots, M \quad (46)$$

The final m values that are gathered for fitness functions to estimate the absolute localization coordinates fall into the anchor environment.

Data set- 100 points, test data- 50 nodes, Validate- 4 positions.Total collected data 200 × 4 = 800 values, accuracy- 95%, sensitivity- 86.5%, classifier- Nuero-Fuzzy,

Classes are sub-divided into four classes according to the standard node distance.

V. RESULTS AND DISCUSSION

The search area is established on every measured target in the preceding section's standard UWB localization algorithm. The proposed method can be implemented within the Fusion Center's existing hardware structure with very moderate changes. The proposed algorithm ELPSO and BPNN, application in UWB indoor localization, was tested in a 10 m x 10 m square simulated area. Two estimators were used to process the nonlinear equations that were generated.

This algorithm was determined to be superior to other widely used algorithms because of its high accuracy and low energy consumption. While this study does not establish how the suggested sensor node localization algorithm works, it demonstrates how it may be used as a viable basis for locating WSNs 3D UWB indoor localization is an extension of 2D. Similarly, suppose a cube region 10 m × 10 m × 10 m, there are four base positions A $(X_a, Y_a, Z_a) = (0, 0, 10)$, B $(X_b, Y_b, Z_b) = (0, 10, 10)$, C $(X_c, Y_c, Z_c) = (10, 10, 10)$, and D $(X_d, Y_d, Z_d) = (10, 0, 10)$ located in it in the same. The configuration of 3D indoor localization is shown in Fig 10. The 50 target positions (x, y, z) are uniformly distributed during the test. For every target, the optimization step is consistent with the two-dimensional case.

Velocity and mobilization of particles near to the anchors and nearby sensors showing very less error when compared with other target nodes in both the cases of measurement 2D and 3D and the co-ordinate values of localization error values are shown in table 1 and table 2.
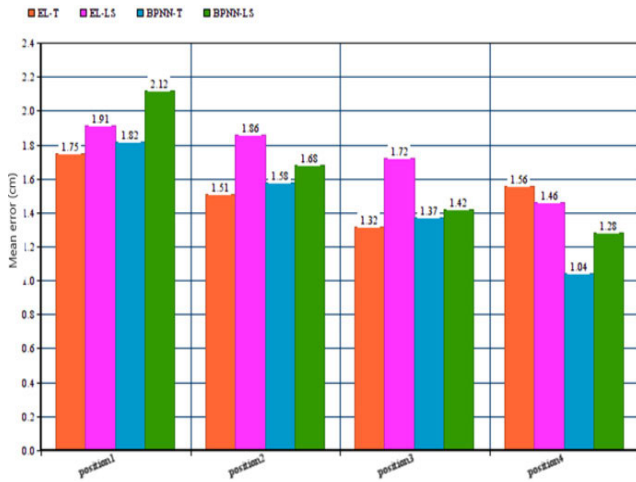
FIGURE 17. Comparative analysis of various algorithms at various positions.

TABLE 3. Co-ordinate values of Localization of 3D positioning.

Optimal technique – method	Movement position	Transmission Range	Max localization Error-cm	Min localization Error-cm	Average LE cm	Total number of located nodes
ELPSO-(T)	1	100M	3.964	0.4320	1.75	50
	2	100M	3.2462	0.3214	1.51	50
	3	100M	2.8654	0.2862	1.32	50
	4	100M	3.4632	0.4938	1.56	50
ELPSO-(LS)	1	100M	4.2365	0.3164	1.91	50
	2	100M	4.6432	0.3458	1.86	50
	3	100M	3.7564	0.3244	1.72	50
	4	100M	3.2146	0.3564	1.46	50
PSO-BPNN-(T)	1	100M	3.8492	0.2654	1.82	50
	2	100M	3.3291	0.3216	1.58	50
	3	100M	2.9654	0.2196	1.37	50
	4	100M	2.2132	0.2456	1.04	50
PSO-BPNN-(LS)	1	100M	4.4263	0.3165	2.12	50
	2	100M	3.6419	0.3427	1.68	50
	3	100M	2.9465	0.2696	1.42	50
	4	100M	2.7222	0.2421	1.28	50
GBNN-PSO REF(33)	1	100M	18.20	10.40	13.8	50
	2	100M	9.78	7.32	8.46	50
	3	100M	3.50	1.37	2.72	50
	4	100M	6.42	3.83	5.22	50
NN-MODEL REF(34)	1	100M	10.0	5.8	7.4	50
	2	100M	16.1	9.4	12.0	50
	3	100M	10.7	7.4	9.2	50
	4	100M	14.2	8.6	11.2	50

When we initially measure an object indoors, we create a search space based on that target, similar to a 2D setup for each target. Figs. 11 and 12 Now we have a three-dimensional representation of the search space, represented by an object. The swarm is triggered and distributed randomly in this sphere.

The deployment of beacons has shown Fig. 14 in the above fitness graphs 15 a,b,c,d. the momentum randomly changed to check the localization error from all the 4 positions. A slight variation found in 3rd, 4th position in which the beacons falls in to two measured positions with equi-distance.

The optimized error values of some nodes find in figure 13 and 16 is very low, the mobilization time of beacon respect to anchor node is near by the location of two anchor nodes. Much variation not found in RMSE the moment near to the wall.

The results Fig. 17 showing that there is significant location error concerning anchor placement conditions; this location optimized to minimize localization error. Dynamic momentum of node will change randomly, with Chan algorithm measurement and filtration, further swarm optimization techniques implemented. All location errors find in cm at dynamic conditions to finalize the exact measured value with anchors. A set of unknown nodes perform localization by estimating the distance from different three anchors. The distance from the anchor to an unknown node is calculated using Receive Strength Signal Indicator (RSSI). Generally, PSO has converged earlier to find the optimal solution that makes PSO trap into the local optimal problem.

The least values of error localization found in 3D with back propagation neural network consideration compared with others and shown in figure 18 and mentioned in table 3. The values obtained were comparatively low after the proposed method and showed a slightest variation of 1.02cm. UWB network with indoor localization positioning with the dynamic interpretation of measured value significantly given

good results in hybrid algorithms with 2D and 3D. In the conducted simulations, the density of anchor nodes. A novel method is implemented to decrease the localization error in UWB environment in indoor network with different optimal methods. The work presented in this paper show a considerable improvement in RMSE for node localization, when TDOA approach is used along with neural networks. This the approach works best when the area involved is small and node density is large. This paper presents a simple neural-network orientation-dependent ranging-error model in 3D space. The selected BPNN model required the measured distance and the calculated orientation, elevation and azimuth, as an input. The experimental data and the results when choosing the
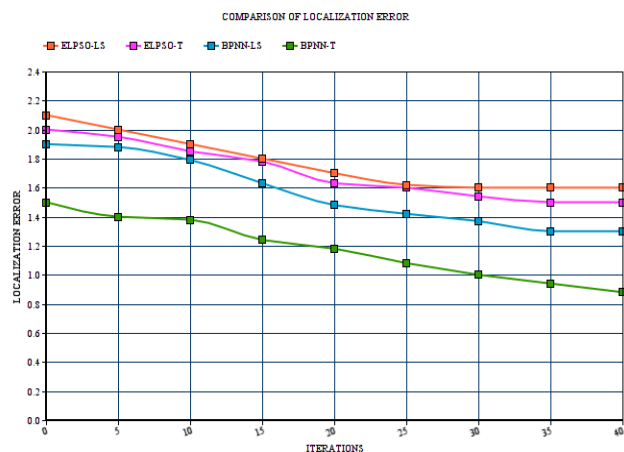
FIGURE 18. Comparison of localization error for all optimal techniques in centimeters.

TABLE 4. Comparison of present state of art with another research.

S. N0	Author	Method	Error range (cm)	Remarks
1	A. Taok et al. 2008	Neural network	Up to 60cm	Very high
2	Chunhua Long et al. 2016	TDOA with Master anchor	15.12-27 cm	Good
3	Tan Wang et al. 2019	TDOA with TOF Hybrid	10-20 cm	Better
4	Proposed	TDOA with Optimal PSO	2.5- 7 cm	

BPNN model configuration are presented and discussed. When testing a different number of neurons in the hidden layer on training data, BPNN model error decreases with a higher number of neurons. The Percentage of training data is 97.5%, validating data-95.29% with accuracy-93.73% by adopting BPNN for the present 3D scenario.

VI. CONCLUSION

The ELPSO algorithm presented in this study uses ultra-wide band (UWB) signals for real-time indoor localization and an entirely new approach to optimization. An optimization problem can be used to solve the interior location problem. Using the ensemble learning technique, a particle learns from its own experience, the experience of its neighbors, and the experience of other swarms. This new learning technique improves indoor location accuracy and helps particles develop an even better and more promising search area. With the current approach, both 2D and 3D UWB indoor location methods using MATLAB can be used. A computa-

tional engine implemented in MATLAB can control both the transmitter and receiver simultaneously. Sound waveforms and related reception filters can be continuously optimized to keep up with the ever-changing monitoring environment. Since wireless sensor networks with many anchor nodes are consistently not distributed, the Chan algorithm is more suitable for rapid moving targets because of a less computing time and relatively stable performance. PSO-based optimization uses hybrid algorithms with Ensemble learning and Back-propagation neural network with localization algorithm of Chan using Kalman filter. PSO with a Back propagation neural network gave the most accurate localization results among all the hybrid combinations. Results after simulation showed PSO-BPNN with tetrahedron 3D given Constance values compared with the other methods. The average inaccuracy is 2.72 cm, which is significant. Compared to the literature review of reference 13,33 and 34 on UWB networks, the minimum localization error is 9cm, and as our optimization process decreases to 2.72 cm, quite a noticeable result.

Comparing different optimizing techniques with metaheuristic algorithms, the localization error with TDOA implementation in UWB indoor environment, error distance decreased much with other methods like GBNN and NN model with Fuzzy and the compared values are shown in table 4. Research on more challenging situations requiring real-time node location will focus on future work because of this original study significance.

REFERENCES

[1] A. Paul and T. Sato, "Localization in wireless sensor networks: A survey on algorithms, measurement techniques, applications and challenges," *J. Sensor Actuator Netw.*, vol. 6, no. 4, p. 24, Oct. 2017, doi: 10.3390/jsan6040024.

[2] T. Van Haute, E. De Poorter, P. Crombez, F. Lemic, V. Handziski, N. Wirström, A. Wolisz, T. Voigt, and I. Moerman, "Performance analysis of multiple indoor positioning systems in a healthcare environment," *Int. J. Health Geograph.*, vol. 15, no. 1, pp. 1–15, Dec. 2016, doi: 10.1186/s12942-016-0034-z.

[3] C. S. Leung, J. Sum, H. C. So, A. G. Constantinides, and F. K. W. Chan, "Lagrange programming neural networks for time-of-arrival-based source localization," *Neural Comput. Appl.*, vol. 24, no. 1, pp. 109–116, Jan. 2014, doi: 10.1007/s00521-013-1466-z.

[4] H. Yan, Y. Xu, and M. Gidlund, "Experimental e-Health applications in wireless sensor networks," in *Proc. WRI Int. Conf. Commun. Mobile Comput.*, vol. 1. Kunming, China, Jan. 2009, pp. 563–567.

[5] F. Zafari, A. Gkelias, and K. K. Leung, "A survey of indoor localization systems and technologies," *IEEE Commun. Surveys Tuts.*, vol. 21, no. 3, pp. 2568–2599, 3rd Quart., 2019.

[6] R. W. Ouyang, A. K.-S. Wong, C.-T. Lea, and M. Chiang, "Indoor location estimation with reduced calibration exploiting unlabeled data via hybrid generative/discriminative learning," *IEEE Trans. Mobile Comput.*, vol. 11, no. 11, pp. 1613–1626, Nov. 2012.

[7] A. Yassin, Y. Nasser, M. Awad, A. Al-Dubai, R. Liu, C. Yuen, R. Raulefs, and E. Aboutanios, "Recent advances in indoor localization: A survey on theoretical approaches and applications," *IEEE Commun. Surveys Tuts.*, vol. 19, no. 2, pp. 1327–1346, 2nd Quart., 2016, doi: 10.1109/COMST.2016.2632427.

[8] I. D. Sumitra, R. Hou, and S. Supatmi, "Study of hybrid localization noncooperative scheme in wireless sensor network," *Wireless Commun. Mobile Comput.*, vol. 2017, pp. 1–10, Mar. 2017, doi: 10.1155/2017/6596943.

[9] S. Tomic, M. Beko, and R. Dinis, "RSS-based localization in wireless sensor networks using convex relaxation: Noncooperative and cooperative schemes," *IEEE Trans. Veh. Technol.*, vol. 64, no. 5, pp. 2037–2050, May 2015, doi: 10.1109/TVT.2014.2334397.

[10] N. Jain, S. Verma, and M. Kumar, "Patch-based LLE with selective neighborhood for node localization," *IEEE Sensors J.*, vol. 18, no. 9, pp. 3891–3899, May 2018, doi: 10.1109/JSEN.2018.2815761.

[11] P. Moravek, D. Komosny, M. Simek, M. Jelinek, D. Girbau, and A. Lazaro, "Investigation of radio channel uncertainty in distance estimation in wireless sensor networks," *Telecommun. Syst.*, vol. 52, no. 3, pp. 1549–1558, Mar. 2013, doi: 10.1007/s11235-011-9522-4.

[12] S. Kianoush, E. Goldoni, A. Savioli, and P. Gamba, "Low-complexity localization and tracking in hybrid wireless sensor networks," *ISRN Sensor Netw.*, vol. 2012, pp. 1–7, Aug. 2012, doi: 10.5402/2012/430169.

[13] L. Zwirello, T. Schipper, M. Harter, and T. Zwick, "UWB localization system for indoor applications: Concept, realization and analysis," *J. Electr. Comput. Eng.*, vol. 2012, pp. 1–11, May 2012, doi: 10.1155/2012/849638.

[14] J.-H. Huh and K. Seo, "An indoor location-based control system using Bluetooth beacons for IoT systems," *Sensors*, vol. 17, no. 12, p. 2917, Dec. 2017, doi: 10.3390/s17122917.

[15] T. Kawai, K. Matsui, Y. Honda, G. Villarubia, and J. M. C. Rodriguez, "Preliminary study for improving accuracy on indoor positioning method using compass and walking detect," in *Advances in Intelligent Systems and Computing*, vol. 620. Cham, Switzerland: Springer, 2018, doi: 10.1007/978-3-319-62410-5_39.

[16] H.-S. Lee, S.-H. Lee, J.-G. Lee, and J.-K. Lee, "Design of beacon-based positioning system using RF and sound wave in smartphone," in *Advances in Computer Science and Ubiquitous Computing* (Lecture Notes in Electrical Engineering), J. Park, V. Loia, G. Yi, and Y. Sung, Eds. Singapore: Springer, 2017, vol. 474.

[17] J. H. Seong, S. H. Lee, W. Y. Kim, and D. H. Seo, "High-precision RTT-based indoor positioning system using RCDN and RPN," *Sensors*, vol. 21, no. 11, p. 3701, 2021, doi: 10.3390/s21113701.

[18] S. M. Sheikh, H. M. Asif, K. Raahemifar, and F. Al-Turjman, "Time difference of arrival based indoor positioning system using visible light communication," *IEEE Access*, vol. 9, pp. 52113–52124, 2021, doi: 10.1109/ACCESS.2021.3069793.

[19] M. Uradzinski, H. Guo, X. Liu, and M. Yu, "Advanced indoor positioning using Zigbee wireless technology," *Wireless Pers. Commun.*, vol. 97, no. 4, pp. 6509–6518, Dec. 2017, doi: 10.1007/s11277-017-4852-5.

[20] T. Wang, H. Xiong, H. Ding, and L. Zheng, "A hybrid localization algorithm based on TOF and TDOA for asynchronous wireless sensor networks," *IEEE Access*, vol. 7, pp. 158981–158988, 2019, doi: 10.1109/ACCESS.2019.2951140.

[21] R. Mazraani, M. Saez, L. Govoni, and D. Knobloch, "Experimental results of a combined TDOA/TOF technique for UWB based localization systems," in *Proc. IEEE Int. Conf. Commun. Workshops (ICC Workshops)*, May 2017, pp. 1043–1048, doi: 10.1109/ICCW.2017.7962796.

[22] F. Mekelleche and H. Haffaf, "Classification and comparison of range-based localization techniques in wireless sensor networks," *J. Commun.*, vol. 12, no. 4, pp. 221–227, Apr. 2017, doi: 10.12720/jcm.12.4.221-227.

[23] M. S. Aruna, R. Ganesan, and A. P. Renold, "Optimized path planning mechanism for localization in wireless sensor networks," in *Proc. Int. Conf. Smart Technol. Manage. Comput., Commun., Controls, Energy Mater. (ICSTM)*, May 2015, pp. 171–177, doi: 10.1109/ICSTM.2015.7225409.

[24] G. Han, H. Xu, J. Jiang, L. Shu, T. Hara, and S. Nishio, "Path planning using a mobile anchor node based on trilateration in wireless sensor networks," *Wireless Commun. Mobile Comput.*, vol. 13, no. 14, pp. 1324–1336, 2014, doi: 10.1016/j.neucom.2016.10.097.

[25] A. R. Kulaib, R. M. Shubair, M. A. Al-Qutayri, and J. W. P. Ng, "An overview of localization techniques for wireless sensor networks," in *Proc. Int. Conf. Innov. Inf. Technol.*, Apr. 2011, pp. 167–172, doi: 10.1109/innovations.2011.5893810.

[26] X. Zhang, J. Fang, and F. Meng, "An efficient node localization approach with RSSI for randomly deployed wireless sensor networks," *J. Electr. Comput. Eng.*, vol. 2016, pp. 1–11, Jan. 2016, doi: 10.1155/2016/2080854.

[27] B. Vandersmissen, "Indoor human activity recognition using high-dimensional sensors and deep neural networks," *Neural Comput. Appl.*, vol. 32, no. 16, pp. 12295–12309, 2020, doi: 10.1007/s00521-019-04408-1.

[28] X. Rao and Z. Li, "MSDFL: A robust minimal hardware low-cost device-free WLAN localization system," *Neural Comput. Appl.*, vol. 31, no. 12, pp. 9261–9278, Dec. 2019, doi: 10.1007/s00521-018-3945-8.

[29] F. Qin, T. Zuo, and X. Wang, "CCpos: WiFi fingerprint indoor positioning system based on CDAE-CNN," *Sensors*, vol. 21, no. 4, p. 1114, Feb. 2021, doi: 10.3390/s21041114.

[30] X. Cai, L. Ye, and Q. Zhang, "Ensemble learning particle swarm optimization for real-time UWB indoor localization," *EURASIP J. Wireless Commun. Netw.*, vol. 2018, no. 1, p. 125, May 2018, doi: 10.1186/s13638-018-1135-0.

[31] R. Samanta, C. Kumari, N. Deb, S. Bose, A. Cortesi, and N. Chakik, "Node localization for indoor tracking using artificial neural network," in *Proc. 3rd Int. Conf. Fog Mobile Edge Comput. (FMEC)*, Apr. 2018, pp. 229–233. [Online]. Available: https://www.researchgate.net/publication/324603083

[32] S. Gharghan, S. Mohammed, A. Al-Naji, M. Abu-AlShaeer, H. Jawad, A. Jawad, and J. Chahl, "Accurate fall detection and localization for elderly people based on neural network and energy-efficient wireless sensor network," *Energies*, vol. 11, no. 11, p. 2866, Oct. 2018, doi: 10.3390/en11112866.

[33] M. S. Mozamir, R. B. A. Bakar, W. I. S. W. Din, and Z. Musa, "GbLN-PSO algorithm for indoor localization in wireless sensor network," *IOP Conf. Ser., Mater. Sci. Eng.*, vol. 769, no. 1, 2020, Art. no. 012033, doi: 10.1088/1757-899X/769/1/012033.

[34] P. Krapež, M. Vidmar, and M. Munih, "Distance measurements in UWB-radio localization systems corrected with a feedforward neural network model," *Sensors*, vol. 21, no. 7, p. 2294, 2021, doi: 10.3390/s21072294.

YEDIDA VENKATA LAKSHMI received the Bachelor of Technology degree from JNTU, Hyderabad, and the Master of Technology degree in electronics and communication engineering from JNTUK. She is currently a Research Scholar at Lovely Professional University, Jalandhar, Punjab, in the field of wireless sensor networks. Her research interests include UWB and soft computing in wireless sensor networks.

PARULPREET SINGH received the Bachelor of Technology degree from IK Gujral Punjab Technical University, Jalandhar, Punjab, the Master of Technology degree in electronics and communication engineering from Lovely Professional University, Phagwara, Punjab, and the Ph.D. degree in the wireless sensor networks from the National Institute of Technology, Jalandhar. He is currently working as an Assistant Professor with the School of Electrical and Electronics Engineering, Lovely Professional University. His research interests include MANETs and soft computing in wireless sensor networks.

MOHAMED ABOUHAWWASH received the B.Sc. and M.Sc. degrees in statistics and computer science from Mansoura University, Mansoura, Egypt, in 2005 and 2011, respectively, and the Ph.D. degree in statistics and computer science from the Channel Program between Michigan State University, East Lansing, MI, USA, and Mansoura University, in 2015. In 2018, he was a Visiting Scholar with the Department of Mathematics and Statistics, Faculty of Science, Thompson Rivers University, Kamloops, BC, Canada. He is currently at the Departments of Computational Mathematics, Science, and Engineering (CMSE), Biomedical Engineering (BME), and Radiology, Institute for Quantitative Health Science and Engineering (IQ), Michigan State University. He is an Associate Professor with the Department of Mathematics, Faculty of Science, Mansoura University. His current research interests include evolutionary algorithms, machine learning, image reconstruction, and mathematical optimization. He was a recipient of the Best Master's and Ph.D. Thesis Awards from Mansoura University, in 2012 and 2018, respectively.

SHUBHAM MAHAJAN (Member, IEEE) received the B.Tech. degree from the Department of Electronics and Communication Engineering, Baba Ghulam Shah Badshah University, and the M.Tech. degree from the Department of Electronics and Communication Engineering, Chandigarh University. He is currently pursuing the Ph.D. degree with Shri Mata Vaishno Devi University (SMVDU), Katra, India. His main research interests include study of wireless communication, optical fiber losses, SS-WDM, FSO, radio over fiber and image processing, multimedia data processing, data mining, and machine learning.

AMIT KANT PANDIT (Senior Member, IEEE) is currently working as an Associate Professor and an Ex-Hod of DECE, Shri Mata Vaishno Devi University (SMVDU), Katra, India. He is a MIR Labs Member and has 19 years of academic experience.

ABEER B. AHMED received the Ph.D. degree. She is a senior academic and business professional. She has entrepreneurial leadership experience in stock market and computer science domains. She is passionate for understanding and positioning technology and products, and educating customers. She is working with the Software Engineering Department, College of Computing and Information Technology, Arab Academy for Science, Technology and Maritime Transport, Cairo. She is also a research professional and a Technical Analyst with prime specialization in the use of intelligent methods to discover hidden patterns within stock data. She has project management skills for research and software development of stock market related product suits. She is the Founder and the Managing Director of Middle East Sentiment Consultant Inc. (MESC). The company's clientele includes major investment corporate in Egypt, Saudi Arabia, and United Arab Emirates.

• • •